16th World Conference on Earthquake, 16WCEE 2017
Santiago Chile, January 9th to 13th 2017
Paper N° 4566
Registration Code: S-1465982491

FEATURES OF LONG-PERIOD GROUND MOTION IN THE KATHMANDU VALLEY DURING THE 2015 GORKHA NEPAL EARTHQUAKE SEQUENCE

M. Shigefuji [1], N. Takai [2], S. Bijukchhen [3], M. Ichiyanagi [4], T. Sasatani [5]

[1] Assistant Professor, Faculty of Human-Environment Studies, Kyushu University, shigefuji@arch.kyushu-u.ac.jp
[2] Associate Professor, Faculty of Engineering, Hokkaido University, tki@eng.hokudai.ac.jp
[3] Graduate Student, Graduate School of Engineering, Hokkaido University, subeg@eng.hokudai.ac.jp
[4] Technical Specialist, Institute of Seismology and Volcanology, Faculty of Science, Hokkaido University, ichimasa@mail.sci.hokudai.ac.jp
[5] Former Professor, Faculty of Engineering, Hokkaido University, sasatani@eng.hokudai.ac.jp

Abstract

On 25 April 2015, the Gorkha earthquake (M_W 7.8) occurred in the Himalayan Range of Nepal. Major damage occurred in central and eastern Nepal. The focal area estimated by U.S. Geological Survey was about 200 km long and 150 km wide, with a large slip area near the Kathmandu Valley. The devastating earthquake was followed by a series of aftershocks: there were four large aftershocks (Mw 6.3~7.3). The aftershock of M_W 6.6 occurred on 25 April 2015 ~80 km northwest of Kathmandu at epicenter near to that of the main shock. The other three large aftershocks were originated ~80 km east of Kathmandu; the aftershock of M_W 6.7 occurred on 26 April 2015 and the aftershocks of M_W 7.3 and M_W 6.3 occurred on 12 May 2015. The aftershock of M_W 7.3 brought about more damages to infrastructures already vulnerable due to the main shock.

The Kathmandu Valley, formed by soft lake sediments of Plio-Pleistocene origin, consists of thick soft sediment below the center of the valley. To understand the site effect of the Kathmandu Valley, we installed continuous recording accelerometers in different parts of the valley. We observed the strong motion records from the 2015 Gorkha Nepal earthquake and the aftershock sequence. In this paper, we examine characteristics of long-period ground motion in the Kathmandu Valley based on the strong motion records from four large aftershocks.

First we examine the velocity Fourier spectra of the radial, transverse, and vertical components at all stations for the four large aftershocks. The velocity Fourier spectra around 0.1 Hz for the three components show nearly the same spectral peaks at all stations including a station on a rock site for three aftershocks except the M_W 6.7 event. In order to investigate the nature of the long-period ground motions with a period of about 10 sec for four aftershocks, we compare time-frequency analysis diagrams of three components at all stations using the multiple filter analysis following Dziewonski *et al.* (1969). The diagrams for three aftershocks show the same peaks around 0.1 Hz just after S-wave arrival on the radial and vertical components.

Next, we investigate these long-period ground motions on the radial and vertical components in detail. Narrow band-pass filters are applied to the radial and vertical velocity waveforms and the particle motions on the radial-vertical plane are drawn. The particle motions of the long-period motion appearing after S-wave arrival has retrograde elliptical motion, which indicates the long-period motion is due to Rayleigh wave.

Finally, we applied the semblance analysis to the narrow band-pass filtered vertical-component velocity waveforms for the M_W 7.3 and M_W 6.3 aftershocks. The phase velocity of the Rayleigh wave was estimated to be about 3 km/s at 10 sec period. We compare these phase velocities with the theoretical ones based on the one-dimensional velocity structure of crust and upper mantle in the Himalayas of eastern Nepal by Monsalve *et al.* (2006). The estimated values are a bit lower than those from Monsalve *et al.* (2006) in the frequency range of 0.05-0.10 Hz.

Keywords: The 2015 Gorkha Nepal Earthquake, Large Aftershocks, Kathmandu Valley, Long-period ground motion

1. Introduction

The Indian Plate underthrusts the Eurasian Plate resulting in occurrence of a number of large earthquakes in Nepal Himalaya. On 25 April 2015, the Gorkha earthquake (M_W 7.8, depth=8.2 km) occurred in the Himalayan Range of Nepal. Major damage occurred not only in Nepal, but also in neighboring countries. The focal area was estimated to be about 200 km long and 150 km wide, with a large slip area under the Kathmandu Valley, by U.S. Geological Survey [1] [2]. The devastating earthquake was followed by a series of aftershocks: more than three hundred fifty of them greater than M 4 and four aftershocks greater than M 6 (Fig. 1, Table 1). The aftershock of M_W 6.6 occurred on 25 April 2015 ~80 km northwest of Kathmandu at epicenter near to that of the main shock. The other three large aftershocks were originated ~80 km east of Kathmandu; the aftershock of M_W 6.7 occurred on 26 April 2015 and the aftershocks of M_W 7.3 and M_W 6.3 occurred on 12 May 2015. The ensuing aftershock activities are concentrated in the eastern part of the rupture area.

The Kathmandu Valley, formed by soft lake sediments of Plio-Pleistocene origin similar to Mexico City, consists of thick soft sediment below the center of the valley [3]. To understand the site effect of the Kathmandu valley, we installed continuous recording accelerometers in different parts of the valley. We observed the strong motion records of the 2015 Gorkha Nepal earthquake sequence [4]. In this paper, we examine characteristics of long-period ground motion in the Kathmandu Valley based on these observed data.

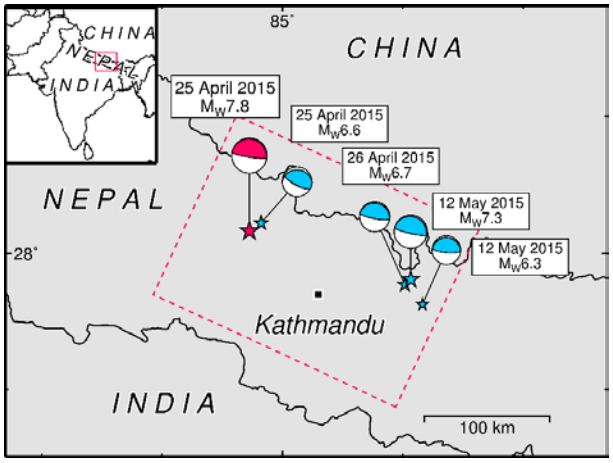

Fig. 1 –Location map of the epicenters of the 2015 Gorkha earthquake and the large aftershocks (M >6). The fault plane shown with the red rectangle and the focal mechanisms are estimated by U.S. Geological Survey (2015) [1] [2].

Table 1 – Source parameters of the main shock and the large aftershocks (M_W >6) [1].

Origin time (UTC)		Latitude [deg.]	Longitude [deg.]	Depth [km]	M_W	Epicentral district
2015/04/25	06:11:26.0	28.23	84.73	8.2	7.8	Gorkha
2015/04/25	06:45:21.3	28.22	84.82	10.0	6.6	Gorkha
2015/04/26	07:09:10.7	27.77	86.02	22.9	6.7	Dolakha
2015/05/12	07:05:19.7	27.81	86.07	15.0	7.3	Dolakha
2015/05/12	07:36:54.5	27.63	86.16	15.0	6.3	Dolakha

2. Strong-motion observation array in the Kathmandu Valley

We installed continuous recording accelerometers in four different parts of the Kathmandu Valley on 20 September 2011 to study the site effect of the valley. The location map of strong-motion arrays is shown in Fig. 2. Four stations were established along a west-east profile of the valley (Array A: KTP, TVU, PTN and THM; the length of about 10 km). On 5 May 2015, 10 days after the main shock, four stations were added along a north-south profile to investigate deep underground structure and aftershock activity (Array B: RNB, PPR, KPN and BKT). A total of eight stations distributed within a radius of about 7 km had been operated since 5 May 2015 to August, 2015. The aftershocks of M_W 6.6 and M_W 6.7 were observed by Array A and those of M_W 7.3 and M_W 6.3, by both the arrays. The KTP site is on the hard rock and the other sites, on the lake sediment.

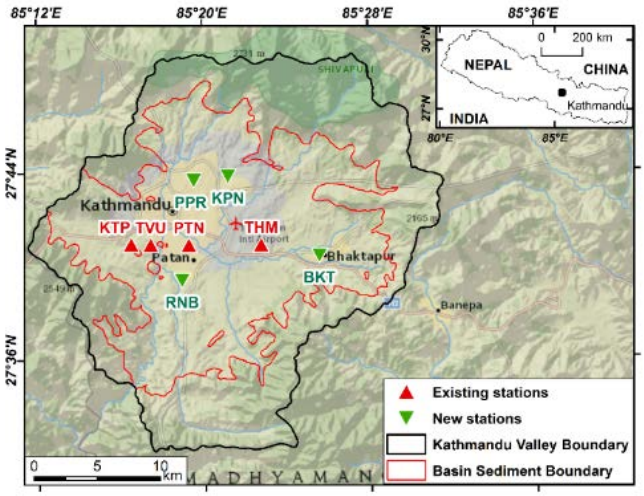

Fig. 2 – Location map of two strong-motion arrays in the Kathmandu Valley [4]. Red triangles: Array A, and green triangles: Array B. For Array A and B, see the text.

3. Strong ground motion records during the aftershocks of the 2015 Gorkha earthquake

We examine the velocity waveforms and velocity Fourier spectra of the radial, transverse, and vertical components at all stations for the four aftershocks; the time window of the spectral analysis is about 80 sec. Figs. 3 and 4 show the observed velocity waveforms and the velocity Fourier spectra for the M_W 7.3 aftershock as an example. The KTP records are considered as reference in order to examine effects of lake sediments on seismic motion. The records at the sedimentary sites have large peak amplitudes than those of the KTP (Fig. 3). The velocity Fourier spectra of the sedimentary sites show significant amplification in the frequency range of 0.2-1.0 Hz compared with the KTP spectrum; however, the spectral peaks and predominant frequencies are different from site to site. On the other hand, the spectra around 0.1 Hz on the three components show nearly the same spectral peaks at all stations including KTP. This demonstrates that long-period (~10 sec) ground motions exist on all three components.

In order to investigate the appearance and nature of the long-period ground motions with a period of about 10 sec (0.1 Hz) for four aftershocks, we compare time-frequency analysis diagrams of three components at all stations for the four aftershocks using the multiple filter analysis following Dziewonski *et al.* (1969) [5]. Fig. 5 shows time-frequency diagrams of KTP as an example. The diagrams for three aftershocks except the M_W 6.7 event show the same peaks around 0.1 Hz just after S-wave arrival on the radial and vertical components; the diagrams of the M_W 6.7 event are different from those of the other events. The long-period motions on transverse component are not clearly observed except the M_W 6.6 and M_W 7.3 events. The KTP site is considered to be a rock site, therefore the above features suggest that these long-period ground motions were excited outside the

Kathmandu Valley. In the next section, we investigate these long-period ground motions on the radial and vertical components in detail.

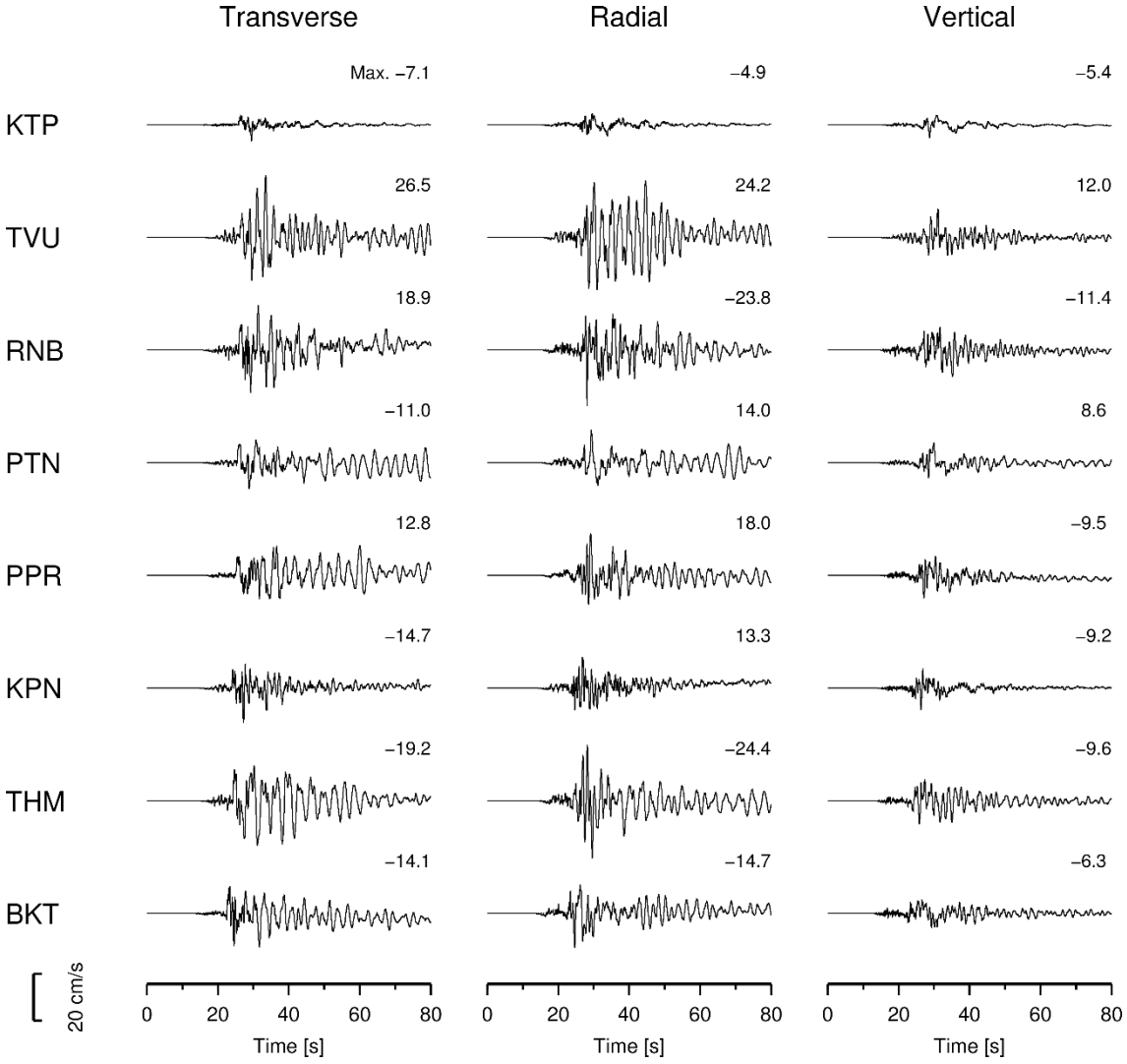

Fig. 3 – Observed velocity waveforms of the largest aftershock on 12 May 2015 (M_W 7.3). These have been corrected for the sensor-response. KTP is a rock site and the others are soft sedimentary sites.

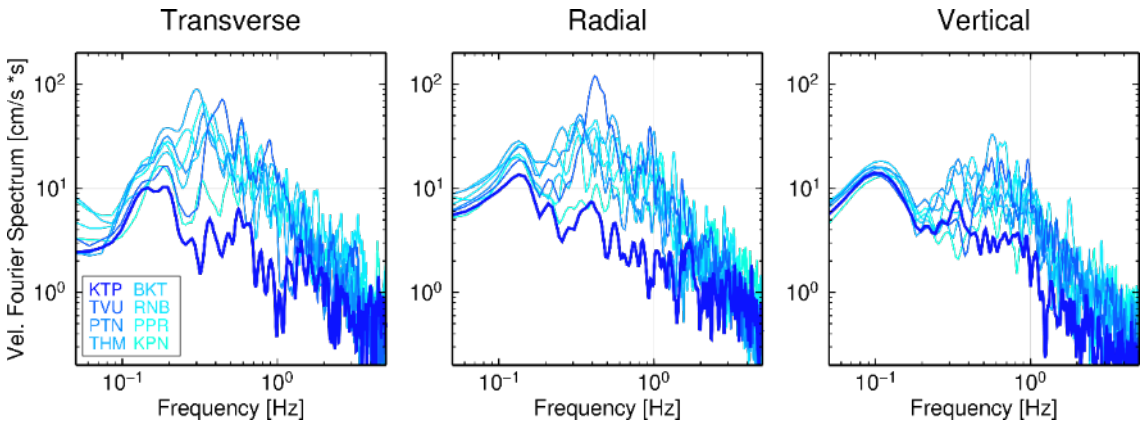

Fig. 4 – Fourier spectra at eight stations for the velocity waveforms shown in Fig.3 observed during the largest aftershock (M_W 7.3) on 12 May 2015.

25 April 2015, M_W 6.6

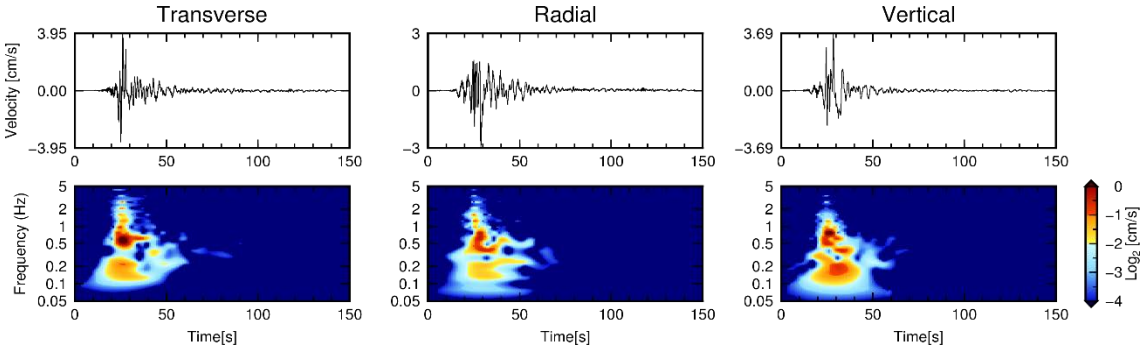

26 April 2015, M_W 6.7

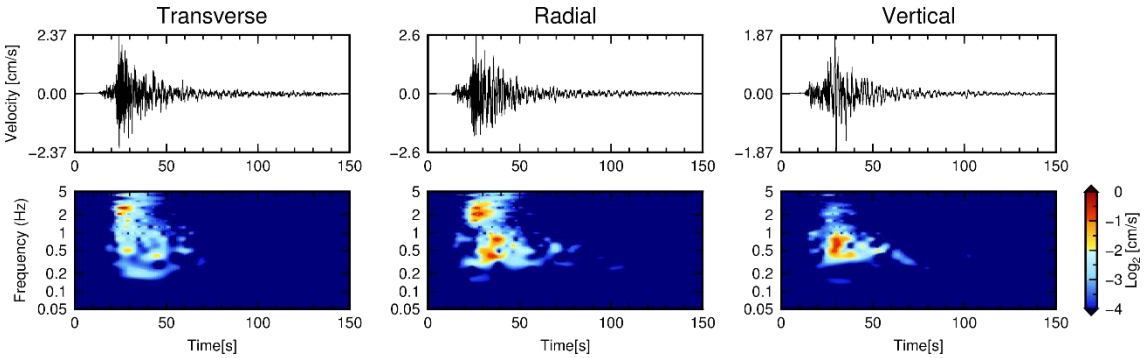

12 May 2015, M_W 7.3

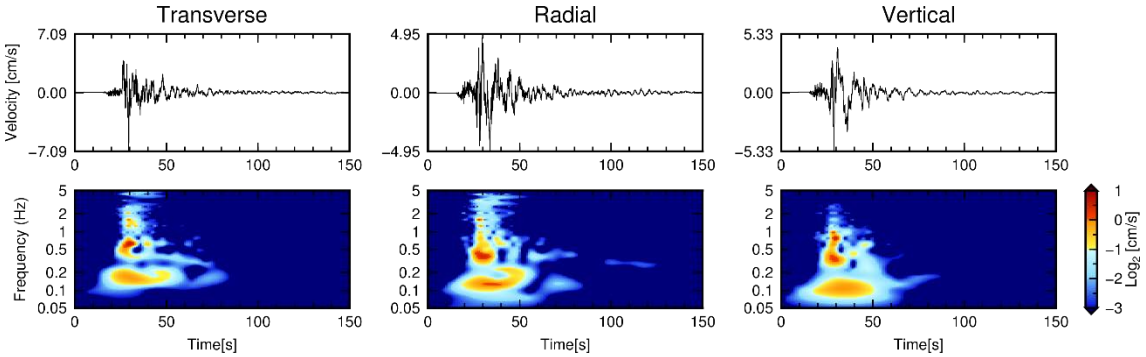

12 May 2015, M_W 6.3

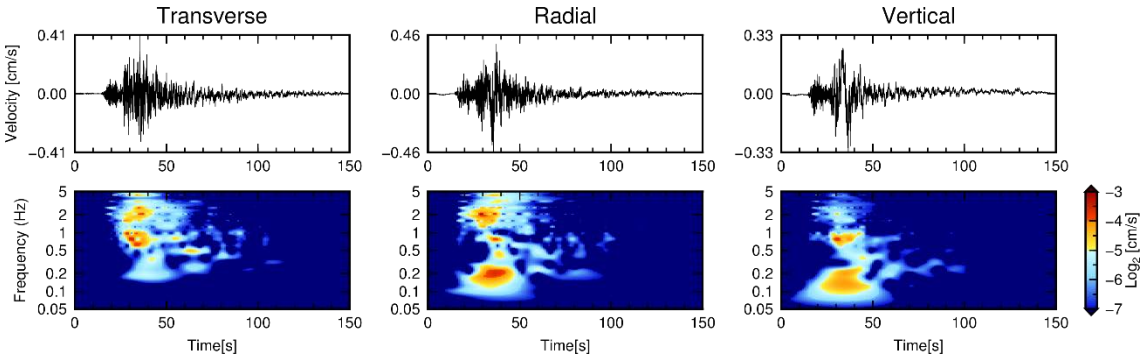

Fig. 5– Observed velocity waveforms (top) and the time-frequency analysis diagrams (bottom) for the four large aftershocks (M_W 6.6, M_W 6.7, M_W 7.3 and M_W 6.3 events) at KTP.

4. Characteristics of the long-period ground motions in the Kathmandu Valley

We estimated the characteristics of the long-period ground motions in the Kathmandu Valley using M_W 7.3 and M_W 6.3 aftershock records obtained from the eight stations (Array A and B). Narrow bandpass filters are applied to the radial and vertical velocity waveforms and the particle motions on the radial-vertical plane are drawn. Fig. 6 shows the results for the central frequency 0.1 Hz at KTP. The particle motions of the long-period waves appearing at the time width of 30 – 40 sec after S-wave arrival has retrograde elliptical motion indicating the presence of Rayleigh wave in the long period motion. This shows that Rayleigh waves of about 10 sec period propagated in the Kathmandu Valley during the large aftershocks except M_W 6.7 event.

In addition, we estimate the apparent velocity and arrival direction of long-period Rayleigh waves using the semblance analysis [6]. The narrow-bandpass filters for the frequency range of 0.05 to 0.15 Hz are applied to the vertical component velocity waveforms at seven stations on the sedimentary sites. Fig. 7 shows the results of the semblance analysis for the case of the central frequency of 0.1 Hz. The semblance analysis shows that the long-period Rayleigh waves have the phase velocity of about 3 km/sec and they arrived from the epicenter.

Fig. 8 shows the phase velocities of Rayleigh waves obtained from the results of the semblance analysis for the M_W 7.3 and M_W 6.3 aftershocks. The variation of the estimated phase velocities below 0.1 Hz is small, but is large above 0.1 Hz. The latter might be caused by overlapping of S-wave with the surface wave. We compare these phase velocities with the theoretical ones based on the one-dimensional velocity structure of crust and upper mantle in the Himalayas of eastern Nepal by Monsalve *et al.* (2006) [7]. The estimated values are lower than those from Monasalve *et al.* (2006) [7] in the frequency range of 0.05-0.10 Hz. This comparison suggests that the S-wave velocity of the top layer of the crust has a bit slower than that from Monsalve *et al.* (2006) [7].

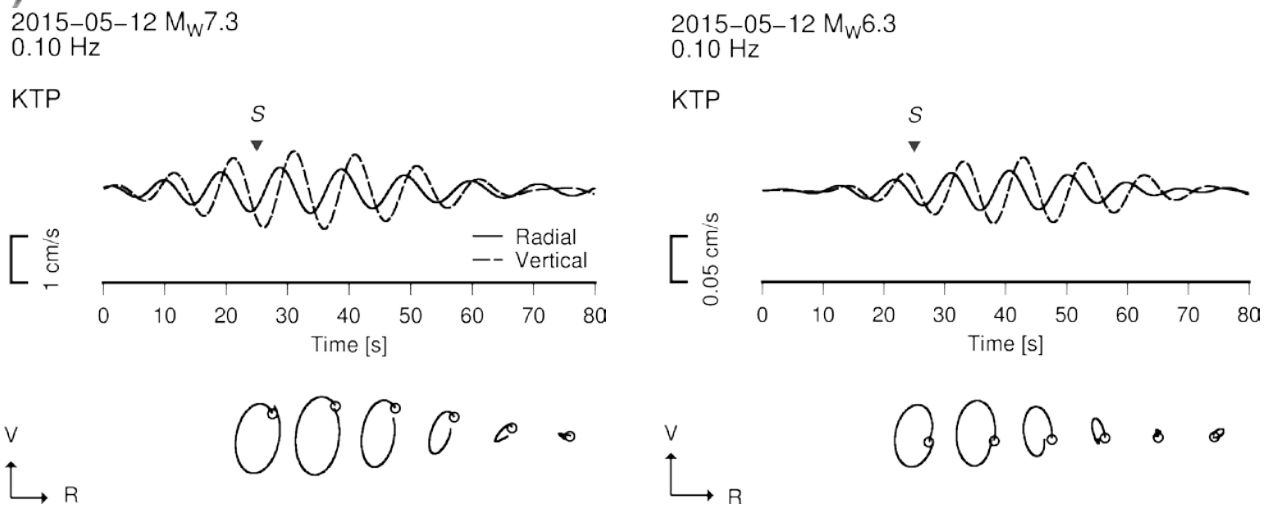

Fig. 6 – Bandpass filtered velocity waveforms and particle motions on the vertical-radial plane at KTP. Narrow band-pass filter is applied with the central frequency of 0.10 Hz. Left: M_W 7.3 aftershock on 12 May 2015, Right: M_W 6.3 aftershock on 12 May 2015. The particle motions are shown for every 10 sec; the starting points are indicated by a small circle.

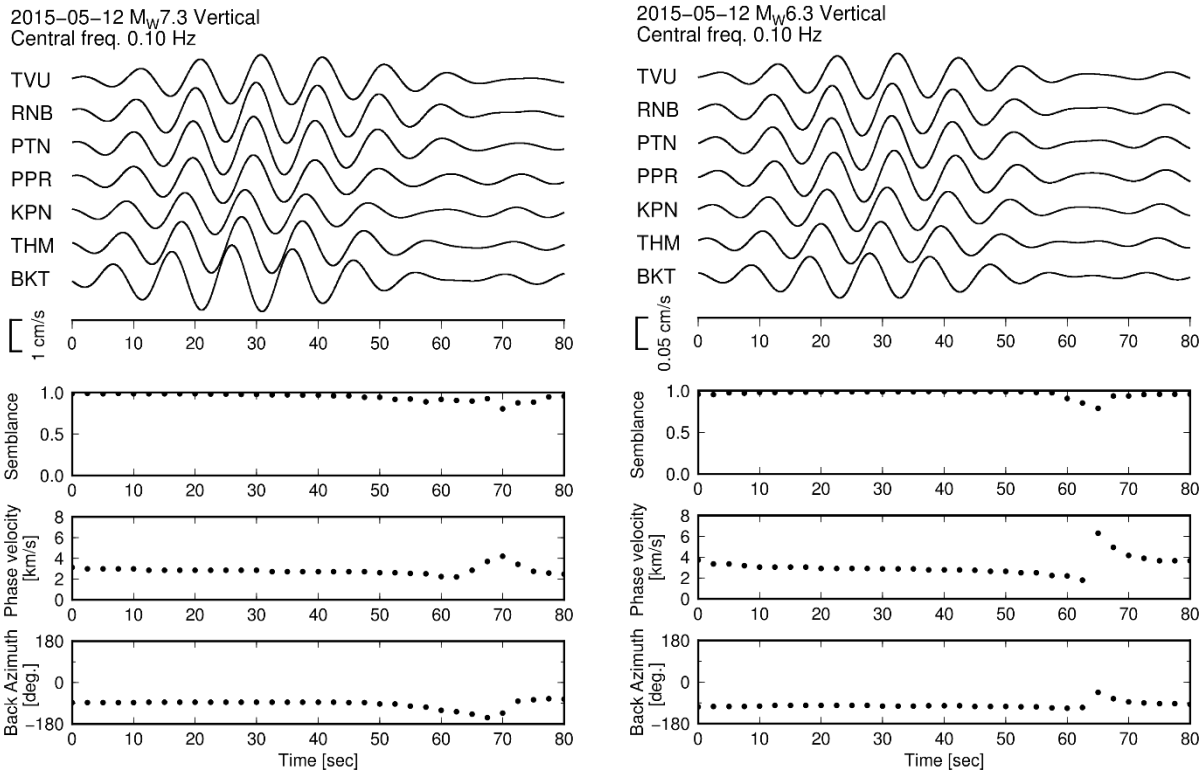

Fig. 7 – Results of semblance analysis. Top: the band-pass filtered velocity waveforms with the central frequency of 0.10 Hz. From the second to the bottom; semblance value, phase velocity, and back azimuth (arrival direction). Left: M_W 7.3 aftershock on 12 May 2015, Right: M_W 6.3 aftershock on 12 May 2015.

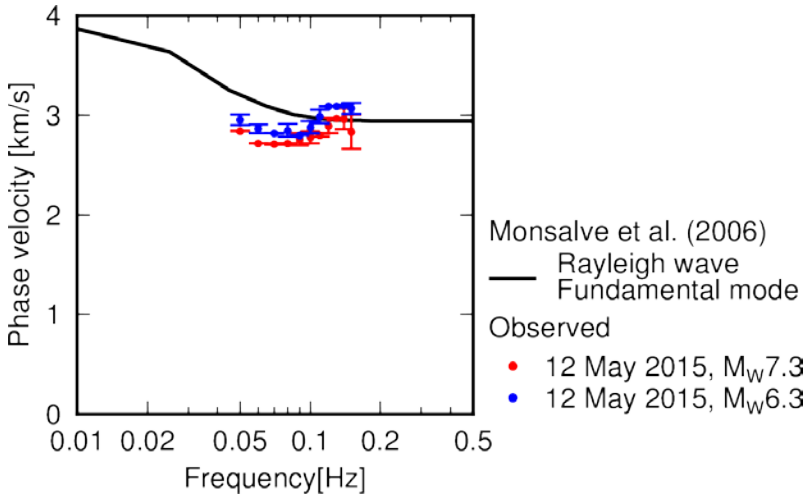

Fig. 7 – Comparison of the estimated phase velocities with the theoretical ones. The circles and the vertical bars indicate the mean values and the standard deviations. Red and blue colors indicate the estimated values from the semblance analysis using M_W 7.3 and M_W 6.3 aftershock records. Black thick curve is the theoretical phase velocity curve for the fundamental-mode Rayleigh wave based on the crustal structure by Monsalve *et al.* (2006) [7].

5. Conclusions

We analysed the long-period strong ground motions in the Kathmandu Valley during the large four aftershocks (M>6) of the 2015 Gorkha Nepal earthquake. We found that the Rayleigh waves with the period around 10 sec appeared soon after S-wave arrival during the three aftershocks except the M_W 6.7 event. The phase velocity of these Rayleigh waves, estimated by semblance analysis, are about 3 km/s at 10 sec period. For further work we will analyse the site effect of the Kathmandu Valley by using these aftershocks and construct a 3-D velocity structure of the valley.

6. Acknowledgements

A part of this study was supported by the Grant-in-Aid for Scientific Research No. 23404005, 15H05793, 16K16370 from MEXT of Japan, Heiwa Nakajima Foundation, Obayashi Foundation, and MEXT of Japan's Earthquake and Volcano Hazards Observation and Research Program, JST of Japan's J-RAPID Program, and JICA-JST SATREPS Program. Grateful thanks to Dr. MR. Dhital, Y. Dhakal, S. Ghimire, Messrs. S. Rajaure, K. Sawada, H. Okajima, Y. Miyahara and M. Aoki. We used the Generic Mapping Tools [8] for drawing the part of the figures.

7. References

[1] U.S. Geological Survey (2015): http://earthquake.usgs.gov/earthquakes/browse/significant.php?year=2015. Accessed 15 October 2016.

[2] Hayes GP, Briggs RW, Barnhart WD, Yeck WL, McNamara DE, Wald DJ, Nealy JL, Benz HM, Gold RD, Jaiswal KS, Marano K, Earle PS, Hearne MG, Smoczyk GM, Wald LA, Samsonov SV (2015): Rapid characterization of the 2015 Mw 7.8 Gorkha, nepal, earthquake sequence and its seismotectonic context. *Seismological Research Letters*, **86** (6), 1557–1567.

[3] Moribayashi S, Maruo Y (1980): Basement topography of the Kathmandu Valley, Nepal: An application of gravitational method to the survey of a tectonic basin in the Himalayas. *Journal of the Japan Society of Engineering Geology*, **21**, 80-87.

[4] Takai N, Shigefuji M, Rajaure S, Bijukchhen S, Ichiyanagi M, Dhital MR, Sasatani T (2016): Strong ground motion in the Kathmandu Valley during the 2015 Gorkha, Nepal, earthquake. *Earth, Planets and Space*, **68** (10).

[5] Dziewonski A, Bloch S, Landisman M (1969): A technique for the analysis of transient seismic signals. *Bulletin of the Seismological Society of America*, **59**, 427-444.

[6] Neidell NS, Taner MT (1970): Semblance and other coherency measures for multichannel data. Geophysics, **36**, 482-497.

[7] Monsalve G, Sheehan A, Schulte-Pelkum V, Rajaure S, Pandey MR, Wu F (2006): Seismicity and one-dimensional velocity structure of the Himalayan collision zone: Earthquakes in the crust and upper mantle. *Journal of Geophysical Research: Solid Earth*, **111**, B10301.

[8] Wessel P, Smith W H F (1991): Free software helps map and display data. *Eos, Transactions American Geophysical Union*, **72**, 441-441.